

Effects of external intermittency and mean shear on the spectral inertial-range exponent in a turbulent square jet

J. Zhang,¹ M. Xu,² A. Pollard,³ and J. Mi^{1,*}

¹State Key Laboratory of Turbulence & Complex Systems, College of Engineering, Peking University, Beijing 100871, China

²Marine Engineering College, Dalian Maritime University, Dalian 116026, China

³Department of Mechanical and Materials Engineering, Queen's University at Kingston, Ontario, Canada K7L-3N6

(Received 26 January 2013; published 14 May 2013)

This study investigates by experiment the dependence of the inertial-range exponent m of the streamwise velocity spectrum on the external intermittency factor γ (\equiv the fraction of time the flow is fully turbulent) and the mean shear S in a turbulent square jet. Velocity measurements were made using hot-wire anemometry in the jet at $15 < x/D_e < 40$, where D_e denotes the exit equivalent diameter, and for an exit Reynolds number of $Re = 50\,000$. The Taylor microscale Reynolds number R_λ varies from about 70 to 450 in the present study. The TERA (turbulent energy recognition algorithm) method proposed by Falco and Gendrich [in *Near-Wall Turbulence: 1988 Zoran Zarić Memorial Conference*, edited by S. J. Kline and N. H. Afgan (Hemisphere Publishing Corp., Washington, DC, 1990), pp. 911–931] is discussed and applied to estimate the intermittency factor from velocity signals. It is shown that m depends strongly on γ but negligibly on S . More specifically, m varies with γ following $m = m_t + (\ln \gamma^{-0.0173})^{1/2}$, where m_t denotes the spectral exponent found in fully turbulent regions.

DOI: [10.1103/PhysRevE.87.053009](https://doi.org/10.1103/PhysRevE.87.053009)

PACS number(s): 47.27.-i

I. INTRODUCTION

The Kolomogrov 1941 theory [1], which is often referred to as K41, has unveiled some intrinsic features of homogeneous isotropic turbulence. One result from K41 is the “ $-5/3$ ” law [2], i.e., the energy spectrum in the inertial range (IR) follows a power relationship,

$$E(k) = C\varepsilon^{2/3}k^{-5/3}, \quad (1)$$

where $E(k)$ is the energy spectrum density function, C is the universal Kolmogorov constant (≈ 1.5) for three-dimensional spectra and the Obukhov-Corrsin constant (≈ 0.4) for one-dimensional spectra (see, e.g., Sreenivasan [3,4] or Pope [5]), ε is the energy dissipation rate, and k is the wave number. The $-5/3$ power law, which has been verified in numerous experimental studies for turbulent flows over “high” Reynolds numbers [6–8], indicates that turbulence energy is transferred from large- to small-scale fluctuations without energy dissipation within the IR. However, the hypotheses for the $-5/3$ law [1] (also see Ref. [9]) are strict so that this power law needs some modifications for flows encountered under common laboratory experimental conditions. For example, the scaling exponent [the absolute value of the exponent of k in Eq. (1)], denoted as m , is found to deviate from $5/3$ in many studies [10–16].

Moreover, the deviation of the scaling exponent (m) from $5/3$ may be caused by insufficiently high Reynolds number, flow anisotropy, or possibly other factors. Mydlarski and Warhaft [16] found the Reynolds number dependence of m in grid turbulence and obtained

$$m = (5/3)(1 - 3.15R_\lambda^{-2/3}) \quad \text{for } 50 \leq R_\lambda \leq 473,$$

where $R_\lambda = (\langle u^2 \rangle^{1/2} \lambda / \nu)$ is the Taylor microscale Reynolds number and $\lambda = (\langle u^2 \rangle^{1/2} / \langle \partial u / \partial x \rangle^2)^{1/2}$ is the Taylor microscale

representing the viscosity-dependent largest-scale eddies. Later, Gamard and George [17] confirmed the result of Mydlarski and Warhaft [16] by deriving a theoretical solution of the R_λ - m relationship for grid turbulence. More recently, the experimental investigations [18,19] were performed on the Reynolds number dependence of m and also for small scales in grid turbulence. Kuznetsov *et al.* [20] investigated the fine-scale structure in intermittent shear flows and noted the dependence of m on the external intermittency factor γ . Specifically, γ is a measure of “external intermittency” [20–22] or “large-scale intermittency” [23], which is related to the turbulent or nonturbulent interfaces [21]. Internal or small-scale intermittency is related to the energy dissipation rate of small-scale turbulence, which will not be considered in this paper. Mi and Antonia [23] discussed the impact of γ on m at $x/D_e = 40$ of a turbulent round jet and discovered that m is also influenced by the mean shear rate S . Especially, they noted that R_λ has a small influence on m when compared to those of the intermittency factor γ and the mean shear rate S . They observed that $m \approx 1.5$ along the jet centerline at $Re = 16\,000$, where $\gamma = 1$ and $S = 0$.

The scaling exponent m , as an intrinsic property of turbulence, is believed to be affected by the local status of the flow. Likewise, the structure function f_n , another important intrinsic characteristic, is also found dependent on Re and the mean shear (see, e.g., Shen and Warhaft [24], and Jiang *et al.* [25]). So far, R_λ , γ , and S have been found to influence m in anisotropic turbulent flows such as wakes and jets. Recently, Xu *et al.* [26] have experimentally validated the R_λ - m relationship obtained for grid turbulence by Mydlarski and Warhaft [16] in a turbulent square jet. The present study considers the same square jet data set obtained during that experimental campaign with a focus on the individual effects of γ and S on m . In other words, the present work investigates the dependence of m on the large-scale intermittency γ and the mean shear S across the jet. Although Mi and Antonia [23] have already reported a similar investigation based on scalar

*Corresponding author: jcmi@coe.pku.edu.cn

signals in a turbulent round jet, an investigation directly based on the velocity signal is needed to examine or extend the results. The choice of a turbulent square jet would further validate the results from a round jet. Also, the effects of γ and S on m are important since, as shown later, the influence of S on m is negligible, a result that contradicts Mi and Antonia [23]. This investigation should be fundamentally important since revealing the relationship between γ and m , i.e., the interactions between flow profiles and the intrinsic characteristics, may lead to some physical insights into the turbulence evolution in this seldom interrogated region of a jet.

The rest of this paper is organized as follows. The experimental setup is briefly described in Sec. II. The data processing methods, including the high-frequency noise filtering scheme and the intermittency detection methods are documented and discussed in Sec. III. In Sec. IV, the intermittency profile for the present square jet is presented and a relationship between m and γ is proposed to assist in evaluating the influence of large-scale nonturbulent motion with distance from the jet exit as well as in the jet lateral direction. Conclusions drawn from the current work are provided in Sec. V.

II. EXPERIMENTAL SETUP

The experimental setup details are described in Ref. [26] and are briefly repeated here. The square jet issued from a square duct whose dimensions were 25 mm (side length, H) \times 25 mm \times 2000 mm (duct length) and the equivalent diameter $D_e [\equiv 2(A/\pi)^{1/2}]$ was 28.2 mm [Fig. 1(b)]. Figure 1(b) also shows the coordinate definition. For breaking up the large-scale structures and reducing the turbulence intensity, the airflow was conditioned in a settling chamber with three air filters before entering the square duct [Fig. 1(a)]. A square plate of $100H$ was attached to the pipe exit to eliminate the perturbations upstream from the exit. Room temperature was $22.0^\circ\text{C} \pm 0.1^\circ\text{C}$ during the experiment.

The measurements were conducted over the range $0 \leq x/D_e \leq 40$, where x is the downstream distance from the nozzle exit. The streamwise mean velocity U_j at the center of the square exit varied from 4.2 to 26.4 m/s, which corresponds to Reynolds number $\text{Re} = U_j D_e / \nu = 8000\text{--}50\,000$. Velocity signals were obtained using an Aupsex single hot-wire sensor (tungsten wire of diameter $d_w = 5\ \mu\text{m}$ and length $l_w = 1\ \text{mm}$) that operated at an overheat ratio of 1.5. Before each measurement, the hot wire was calibrated against a standard Pitot static tube connected to a digital pressure transducer (Datametrics model 590D-10W-2P1-V1X-4D). The sampling frequency f_s for all measurements was 40 kHz and the cutoff frequency f_c was set to half of f_s according to the Nyquist sampling theorem. A 12-bit A/D converter (National Instruments, 6070E PCI) was used for digitalizing the signals and each signal was recorded for 80 s to ensure statistical convergence of the quantities in the present study.

Xu *et al.* [26] noted that the mean and fluctuating axial velocity data reached asymptotic conditions around $\text{Re} = 50\,000$; thus, those data from that Reynolds number are used here to explore the effects of the external intermittency and mean strain rate on the scaling exponent, m .

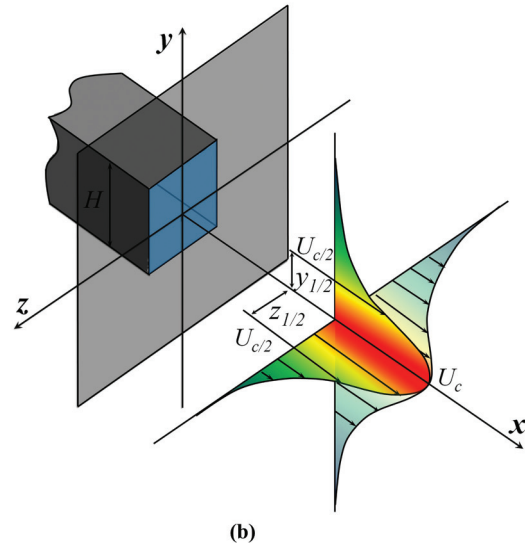
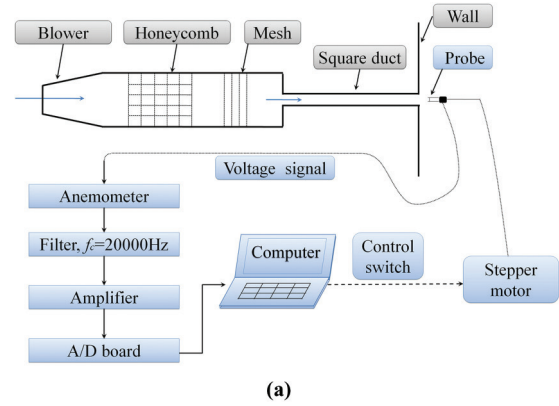


FIG. 1. (Color online) (a) Schematic of the experimental arrangement and (b) three-dimensional square jet nozzle exit, jet notation, and coordinate system.

III. DATA PROCESSING

A. Iterative high-frequency noise digital filter

To remove the high-frequency noise in velocity signals, the iterative digital filter proposed by Mi *et al.* [27] was used. This digital filter obtains the “true” cutoff frequency f_K by iteratively calculating the dissipation rate ε , the Kolmogorov scale η , and the cutoff frequency f_K (for filtering the signal), since these three have the following relationship:

$$\varepsilon_m = \varepsilon[\text{true dissipation}] + \varepsilon_n[\text{noise contribution}] = B\varepsilon, \quad (2)$$

$$\eta_m = [v^3/(B\varepsilon)]^{1/4} = B^{-1/4}\eta, \quad (3)$$

$$f_{\kappa m} = U(2\pi B^{-1/4}\eta)^{-1} = B^{1/4}f_K, \quad (4)$$

where the subscript m means “measured,” n means “noise,” U is the local streamwise mean velocity, and B is a constant reflecting the effect of high-frequency noise and can be determined after the iterative filtering converges. Equations (2)–(4) also describe how the noise affects the three Kolmogorov scales. By calculating and filtering iteratively, the noise contribution can be “squeezed out.” An experimental validation of this method can be found in [28]. Note that this filtering scheme does not affect the IR [28]; i.e., this scheme

does not change the value of the scaling exponent, which is to be investigated below. Also the applications of both the local isotropy assumption and Taylor's hypothesis used to estimate the dissipation rate ε , i.e., $\varepsilon = 15\nu\langle(\partial u/\partial x)^2\rangle$ and $\langle(\partial u/\partial x)^2\rangle = (1/U^2)\langle(\partial u/\partial t)^2\rangle$, do not influence the results and conclusions drawn from the present study.

B. Determination of the intermittency factor

The intermittency factor γ was introduced first by Townsend [29] who considered local isotropy in the turbulent wake of a cylinder. He estimated γ by using the relationship between the measured flatness $F_m(u)$ and the flatness $F_0(u)$ obtained from isotropic grid turbulence: $F_m(u) = \gamma^{-1}F_0(u)$ [29]; however, this method is impracticable when $F_0(u)$ is not available. Thus, some authors have considered alternate methods to determine γ in a turbulent jet; see, for example, Corrsin and Kistler [30], Becker *et al.* [31], Wygnanski and Fiedler [32], Antonia *et al.* [33], Bilger *et al.* [34], Gilliland *et al.* [22], and Mi and Antonia [23] or, from velocity signals [29,30] and scalar signals using probability density function (PDF) methods [22,23,34]. An important component in determining γ from velocity signals is the detector function that is used to determine whether the signal is turbulent or not. Hedley and Keffer [35] surveyed the detector functions proposed before 1974. Falco and Gendrich [36] proposed an intermittency detection method, which they called the turbulent energy recognition algorithm (TERA) and later Zhang *et al.* [37] modified this method by altering the threshold criteria (M-TERA), to improve the stability when detecting γ within a transitional boundary layer.

The TERA method uses $u'\partial u'/\partial t$ as the detection function, and the criterion for turbulence is

$$\left| \frac{u'\partial u'}{\partial t} \right| > C_0 \left(\frac{u'\partial u'}{\partial t} \right)_{\text{rms}}, \quad (5)$$

where u' denotes the velocity fluctuation. The left side of (5) is the time average of the detection function over a predefined time interval Δt and the right side is the criterion (threshold level), where C_0 is a preset threshold constant.

Figures 2(a1)–2(a4) illustrate how the turbulence velocity signals are used to determine the intermittency factor γ using the TERA method. A section of a typical velocity signal is shown in Fig. 2(a1). The specific time $\tau = \lambda = \langle u^2 \rangle^{1/2} = 1/\langle(\partial u/\partial x)^2\rangle^{1/2}$ for this section is about 3 ms and the duration of this signal is about 40 ms. From the calculation of the detector function, $u'\partial u'/\partial t$, the turbulent portion of the signal is well captured; see Fig. 2(a2). Figure 2(a3) shows the time average of $|u'\partial u'/\partial t|$ over a predefined time interval Δt . A more precise delineation of the turbulent signal may be obtained using an indicator function $I(t)$,

$$I(t) = \begin{cases} 1, & \left| \frac{u'\partial u'}{\partial t} \right| > C_0 \left(\frac{u'\partial u'}{\partial t} \right)_{\text{rms}} \quad (\text{signal is turbulent}) \\ 0, & \left| \frac{u'\partial u'}{\partial t} \right| \leq C_0 \left(\frac{u'\partial u'}{\partial t} \right)_{\text{rms}} \quad (\text{signal is nonturbulent}) \end{cases}, \quad (6)$$

as presented in Fig. 2(a4). Thus, the length of the turbulent signal to that of the total signal is the intermittency factor γ . A determination of γ from a real velocity signal using the TERA method is illustrated in Fig. 2(b). A shorter time

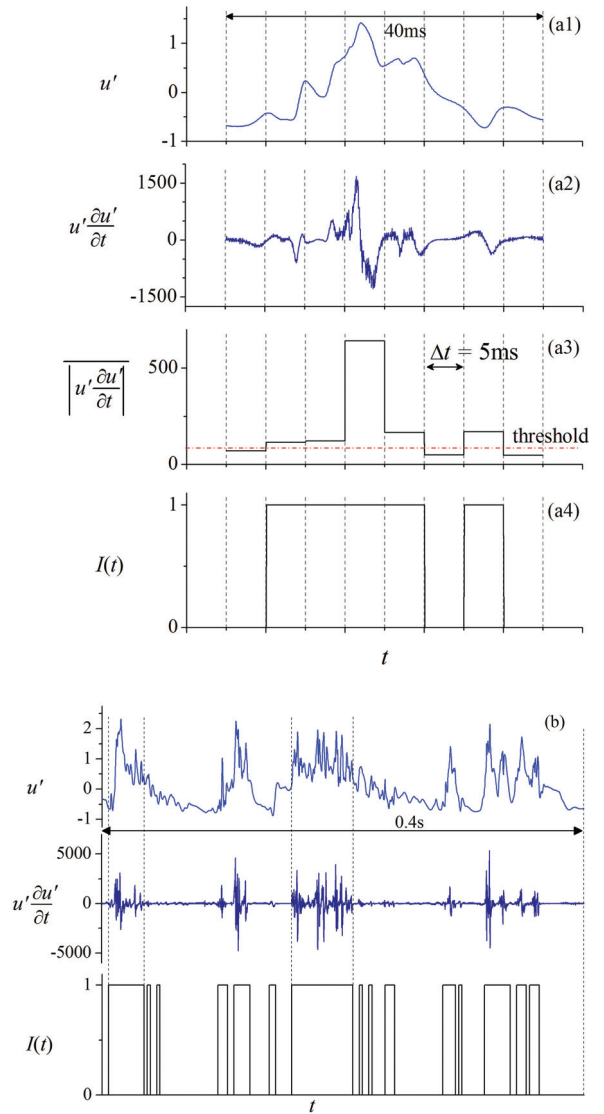


FIG. 2. (Color online) Illustration of the detection procedure. (a1) Time-sequential velocity signal [specific time $\tau = \lambda/\langle u^2 \rangle^{1/2} = 1/\langle(\partial u/\partial x)^2\rangle^{1/2} \approx 3$ ms; the duration is about 40 ms]; (a2) detector function $u'\partial u'/\partial t$ calculated from the signal; (a3) average of the detector function in a predefined time interval $\Delta t = 5$ ms; (a4) determination function $I(t)$ of the signal; and (b) a determination of γ from a real velocity signal (the duration is about 0.4 s).

interval correlates to increased detection sensitivity; however, given that $\Delta t = 1$ ms does not give $\gamma = 1$ at the centerline, and that there is diminished sensitivity for longer time intervals, as can be noted from Fig. 3, $\Delta t = 5$ ms was chosen for the intermittency detection. In fact, the range of the specific time τ for these lateral locations is about 2–4 ms; thus Δt may be set slightly larger than τ . The M-TERA method is similar to TERA but uses $C_M \bar{u}(\partial u'/\partial t)_{\text{rms}}/(u'\partial u'/\partial t)_{\text{rms}}$ as the criterion.

The TERA and M-TERA methods were applied to the current data set for the square jet and the TERA method was found better for detecting γ . As is shown in Fig. 4, at $x = 15D_e$ and $x = 25D_e$ the intermittencies obtained using either TERA or M-TERA are in reasonable accord; however, at $x = 35D_e$ there is significant difference between them. Since γ should

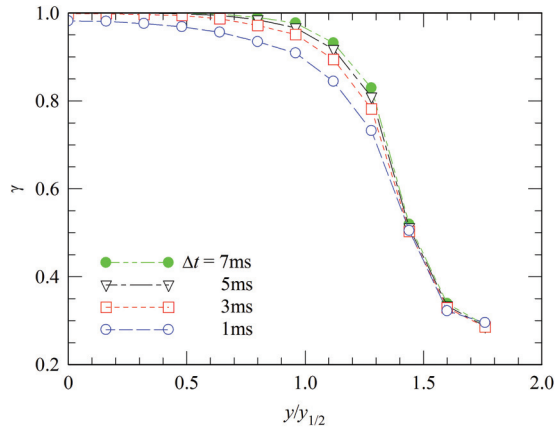


FIG. 3. (Color online) Time interval effect on the intermittency detection.

be close to 1.0 in the region between centerline and the shear layer of the jet, i.e., the turbulence region, it is concluded that M-TERA is probably less reliable than TERA. Thus, the TERA method was applied for detecting γ of the current square jet.

Zhang *et al.* [37] have shown that the detection of the TERA method deviates from the “exact result” when $\gamma < 0.1$ (see their Fig. 5) and this deviation was also observed in the present γ detection (not shown). However, it is worth noting that in the present study the intermittency factors are all above 0.2 so that the TERA method provides reliable results. The present γ detection is confirmed below. Previous studies have shown that the PDF method proposed by Bilger *et al.* [34] provides satisfactory intermittency detections for scalar signals from a turbulent jet [22,23], even when $\gamma < 0.1$. However, due to the directionality of velocity, it can be deduced that the PDF method may not be suitable for a velocity signal while the TERA method may detect intermittency for both velocity and scalar signals since the TERA method detects γ via the intensity of fluctuations. Unfortunately, the scalar field of the present square jet was not measured so it is not possible to compare the performance of the PDF and the TERA methods. The defects of the M-TERA and TERA method mentioned above suggest that further study on the real-time flow energy recognition for jet flow is needed.

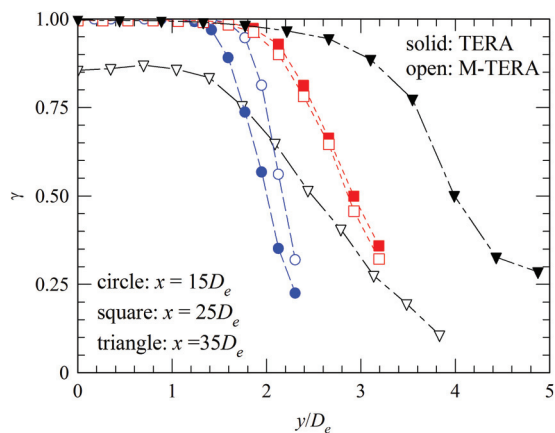


FIG. 4. (Color online) External intermittencies detected by the TERA and M-TERA methods.

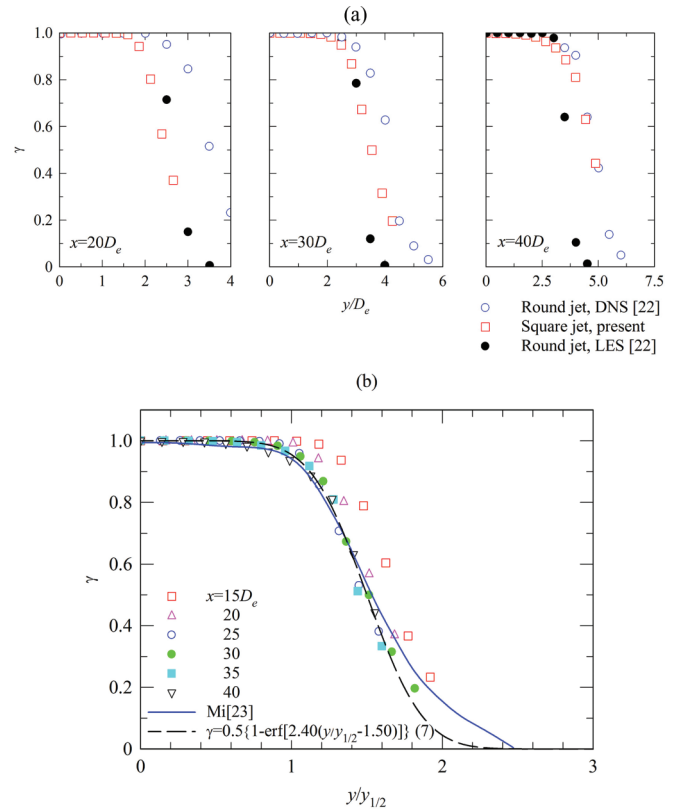


FIG. 5. (Color online) Lateral profiles of the intermittency obtained using the TERA method: (a) Comparison with the DNS and LES results of Gilliland *et al.* [22]; (b) comparison with the results of Mi and Antonia [23] and a fitting for the self-similarity of γ . (Gilliland *et al.* did not provide the corresponding half-width so the abscissae are normalized by (a) the equivalent diameter D_e and (b) the corresponding half-widths, respectively).

IV. PRESENTATION AND DISCUSSION OF RESULTS

A. Intermittency and mean shear in the square jet

According to Mi and Antonia [23], the intermittency and the mean shear are important to the scaling exponent in the IR of a round jet and these two factors are considered below. The variation of γ as a function of lateral and axial locations is

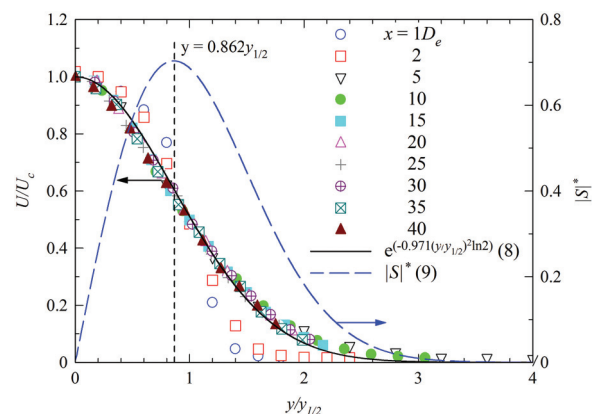


FIG. 6. (Color online) Lateral profiles of normalized mean velocity and mean shear in the square jet.

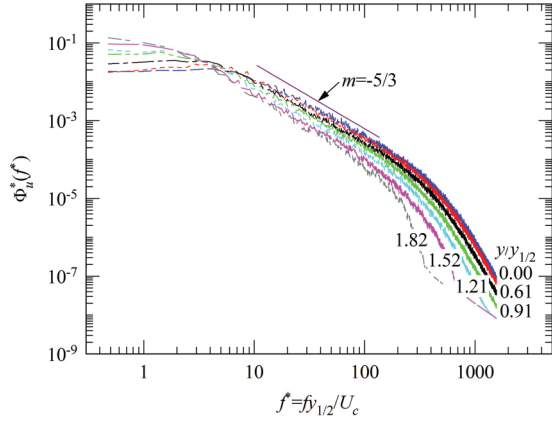


FIG. 7. (Color online) Spectra $\Phi_u^*(f^*)$ of the streamwise velocity at different y locations for $x = 30D_e$.

shown in Figs. 5(a) and 5(b). The TERA threshold constant was set as $C_0 = 0.04$, which provided good agreement between the present far-field ($x/D_e \geq 25$) results and those from Gilliland *et al.* [22] and Mi and Antonia [23]. Note that Gilliland *et al.* presented results for a round free jet obtained using large eddy simulation (LES) and direct numerical simulation (DNS) for $Re = 2400$. They used a synthetic inlet boundary condition. Therefore, the difference in the Re between these data sets is apparent so that different intermittency detection results are expected. Indeed, the present results are close to those of Gilliland *et al.* [22] for $x > 30D_e$, and the differences in the near field are probably due to incomplete development of the simulated jet as well as the synthetic inlet boundary condition. Figure 5(b) indicates that $\gamma \approx 1$ within $y/y_{1/2} \leq 1$ while it drops rapidly to zero at $1 < y/y_{1/2} \leq 2.5$. When normalized

by the half-width of the jet, the intermittency factor exhibits a self-similar characteristic in the far field for $x > 25D_e$. This profile fits a Gaussian error function,

$$\gamma = 0.5\{1 - \text{erf}[2.40(y/y_{1/2} - 1.50)]\}. \quad (7)$$

Figure 6 presents the lateral mean shear, which is obtained from the lateral mean velocity distribution fitted by a Gaussian function,

$$U/U_c = e^{-(y/y_{1/2})^2 \ln 2}. \quad (8)$$

Relative to the intermittency, the mean velocity U reaches self-similarity much earlier ($x > 5D_e$). The normalized mean shear may be defined as

$$|S|^* = (y_{1/2}/U_c) |\partial U / \partial y|, \quad (9)$$

the profile for which is given in Fig. 6, as can be obtained from (8). Mi and Antonia [23] used a different definition for the normalized mean shear (see their Fig. 2):

$$S^* = |\partial U / \partial y| (v / \langle \epsilon \rangle)^{1/2}. \quad (10)$$

We have chosen to use (9) rather than (10) because local isotropy assumption is not expected to work in regions away from the jet centerline. The maximum mean shear occurs at $y = 0.849y_{1/2}$ as may be noted from Fig. 6.

Before turning attention to the effects of the external intermittency and mean shear, the appropriateness of using a stationary hot wire to determine the intermittency can be argued here. Generally speaking, the velocity measurements obtained by a stationary single hot wire may be contaminated by the reverse flow, especially in the outer region of the far field. However, the estimation of γ only requires that the turbulent or nonturbulent flow information be recorded, rather than the velocity vector itself, and so should not be affected by

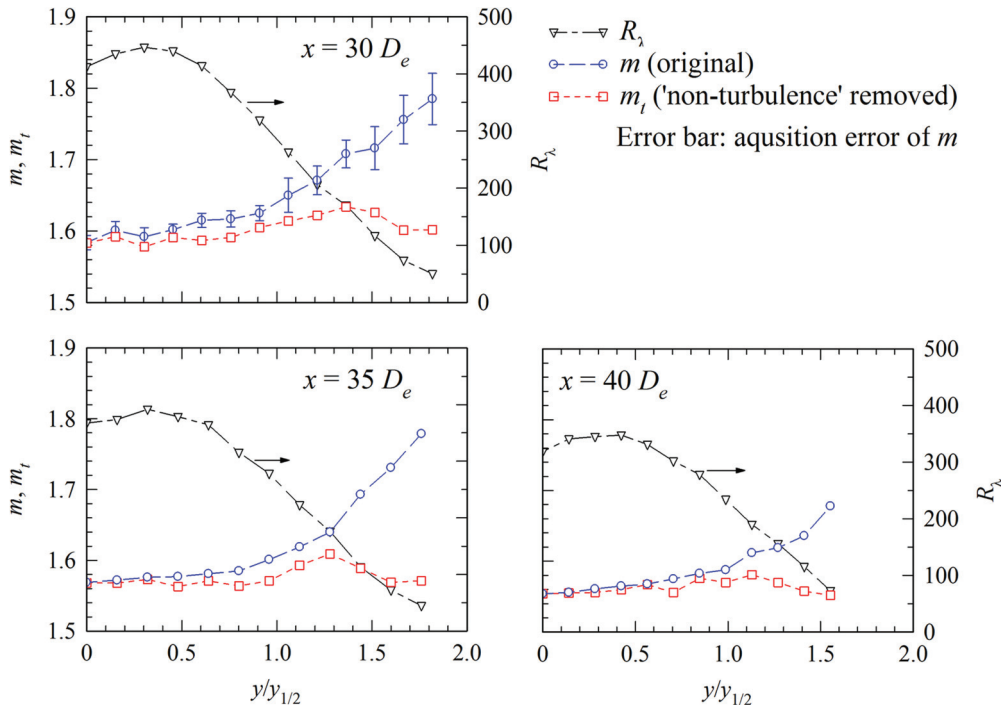


FIG. 8. (Color online) Scaling exponents (m, m_t) obtained from original signals and those excluding the nonturbulent component and the Taylor microscale Reynolds number R_λ at different x locations in the far-field.

the contamination. The contamination also may not influence the scaling exponent since m is almost identical in the spectra of u , v , and w [12]. Furthermore, the lateral mean velocity ($< 0.02U_0$) is negligible at $y/y_{1/2} < 2$ (see Fig. 5.6 in Pope [38]) so that the reverse flow should not affect the conclusions drawn from the present study.

B. Effect of the intermittency and mean shear on the scaling exponent

According to K41, the scaling exponent m should be $5/3$. Yet, the value of m in the current jet flow deviates from $5/3$. This can be seen from spectra, in Fig. 7, of the streamwise velocity u obtained at $x = 30D_e$. Discrepancies are observed in the IR slope for different y locations. It is clear that, as y increases, m grows, i.e., the spectra within the IR become steeper. This is consistent with the observation of Mi and Antonia [23]. Also, their observation is confirmed here that R_λ has a smaller impact on m than does γ or S . Of note, these authors demonstrated (as have Sadeghi and Pollard [39]) that, as y increases, R_λ reduces but m grows. However, Mydlarski and Warhaft [16] found that m decreases as R_λ reduces for their investigation of grid turbulence. Hence it is deduced that the R_λ effect on m is much smaller than that of γ or S , which has been validated in Fig. 8.

The application of the TERA method enables the identification of the nonturbulent component, the removal of which from the original velocity signal allows the dependence of m only on the intermittency to be determined. Figure 8 compares m and m_t , i.e., the scaling exponents with and without the effect of γ , at various y locations for $30 < x/D_e < 40$ along with the lateral distributions of R_λ . It is shown that R_λ varies from about 70 to 450 at different locations. Evidently, m increases significantly with y while m_t does not. More specifically, m changes mildly at $y < y_{1/2}$ and then rapidly increases beyond $y = y_{1/2}$. Note that m and m_t decrease from about 1.6 to about 1.55 on the centerline, where $\gamma = 1$ and $S = 0$, over the region $30 < x/D_e < 40$. According to Refs. [16] and [39], the only factor that could be responsible for the decrease in m along the centerline is R_λ . Indeed, R_λ drops from 412 to 318 over the region $30 < x/D_e < 40$. In addition, with the removal of the nonturbulent component, all the scaling exponents decrease

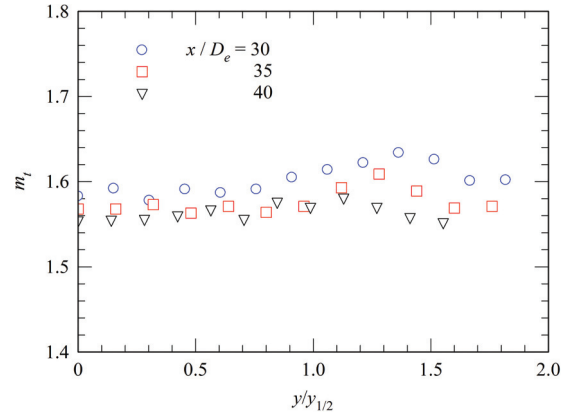


FIG. 10. (Color online) Lateral profiles of the scaling exponent (m_t) of the velocity signal taken out the nonturbulent part.

and the largest diminution occurs at the outermost measured positions.

If the nonturbulent portion of the velocity signal is removed, the obtained signal should be related only to the turbulence (thus m_t) and the spectrum should not be affected by the external intermittency. It follows that the difference

$$\Delta m = m - m_t \tag{11}$$

should result solely from γ . The $\gamma \sim \Delta m$ plots at different downstream locations are presented in Fig. 9. Taking into account the error in the acquisition of m , as the error bar plotted in Fig. 9 indicates, Δm varies with γ according to

$$\Delta m = (\ln \gamma^{-0.0173})^{1/2}. \tag{12}$$

Note that those data from Mi and Antonia [23] are also plotted in Fig. 9.

Figure 10 shows that the lateral profiles of m_t obtained at different x locations enable the effect of mean shear S on m to be examined. If S has a significant impact on m , the variation of m_t (no γ effect) with y should be significant. However, Fig. 10 demonstrates that m_t changes little across the jet. Hence, there is no significant effect of mean shear on m . Moreover, the result of Mi and Antonia [23] also suggests that S has a minor influence on m . They chose the region where $\gamma = 0.95-1$ to study the effect of S so that the γ effect is negligible. However, a maximum of only 5% change in m is observed (see their Fig. 7). Taking into account that γ influences m significantly, it is hard to tell whether or not this 5% change in m is solely caused by the mean shear.

V. CONCLUSIONS

The present study has investigated the effects of the intermittency factor γ and the mean shear S on the spectral scaling exponent m in the self-similar far field ($x = 30-40D_e$) of a turbulent square jet at $Re = 50000$. The TERA method proposed by Falco and Gendrich [36] was used to detect the intermittency in hot-wire velocity signals. It was shown that the lateral distribution of the intermittency factor γ reaches self-similarity in the present jet at $x > 30D_e$ and can be well fitted by the Gaussian error function $\gamma = 0.5\{1 - \text{erf}[2.40(y/y_{1/2} - 1.50)]\}$. It was also found that

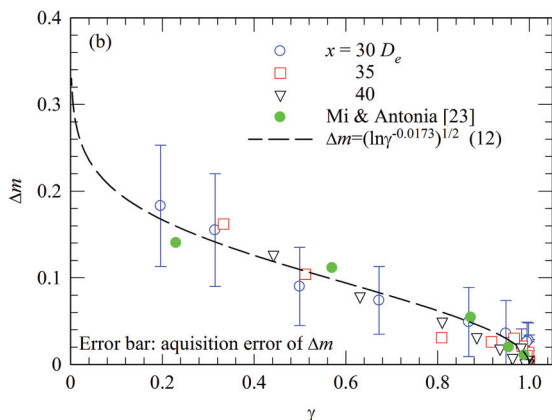


FIG. 9. (Color online) Relationships between Δm and γ at different downstream locations.

the intermittency factor γ has stronger impact on the scaling exponent m than does the Taylor microscale Reynolds number R_λ . The influence of γ on m can be described as

$$\Delta m = m - m_i = (\ln \gamma^{-0.0173})^{1/2},$$

which may be applicable to other jet flows. By comparison, the influence of the mean shear S is apparently negligible.

ACKNOWLEDGMENTS

The support of Nature Science Foundation of China (Grants No. 10921202 and No. 11072005) is gratefully acknowledged. A.P. acknowledges the financial support of the Natural Sciences and Engineering Research Council of Canada. M.X. acknowledges the Fundamental Research Funds for the Central Universities (Grant No. 3132013029).

-
- [1] A. N. Kolmogorov, Dokl. Akad. Nauk SSSR **30**, 299 (1941).
 [2] A. M. Obukhov, Dokl. Akad. Nauk SSSR **32**, 22 (1941).
 [3] K. R. Sreenivasan, *Phys. Fluids* **7**, 2778 (1995).
 [4] K. R. Sreenivasan, *Phys. Fluids* **8**, 189 (1996).
 [5] S. B. Pope, in *Turbulent Flows* (Cambridge University Press, Cambridge, 2000), p. 200.
 [6] H. L. Grant, R. W. Stewart, and A. Moilliet, *J. Fluid Mech.* **12**, 241 (1962).
 [7] A. L. Kistler and T. Vrebalovich, *J. Fluid Mech.* **26**, 37 (1966).
 [8] S. G. Saddoughi and S. V. Veeravalli, *J. Fluid Mech.* **268**, 333 (1994).
 [9] U. Frisch, *Turbulence: The Legacy of A. N. Kolmogorov* (Cambridge University Press, Cambridge, 1995).
 [10] C. J. Lawn, *J. Fluid Mech.* **48**, 477 (1971).
 [11] M. S. Uberoi and P. Freymuth, *Phys. Fluids* **13**, 2205 (1970).
 [12] M. M. Gibson, *J. Fluid Mech.* **15**, 161 (1963).
 [13] P. Bradshaw, D. H. Ferris, and R. F. Johnson, *J. Fluid Mech.* **19**, 591 (1964).
 [14] J. C. Laurence, NACA Report No. 1292, 1956.
 [15] K. R. Sreenivasan, *Proc. R. Soc. London, Ser. A* **434**, 165 (1991).
 [16] L. Mydlarski and Z. Warhaft, *J. Fluid Mech.* **320**, 331 (1996).
 [17] S. Gamard and W. K. George, *Flow, Turbul. Combust.* **63**, 443 (1999).
 [18] M. Ferchichi and S. Tavoularis, *Phys. Fluids* **12**, 2942 (2000).
 [19] B. R. Pearson, P. A. Krogstad, and M. A. Carper, in *Proceedings of the 14th Australasian Fluid Mechanics Conference*, edited by Bassam Dally (Causal Productions Pty, Ltd., Adelaide, Australia, 2001), pp. 167–170.
 [20] V. R. Kuznetsov, A. A. Praskovsky, and V. A. Sabelnikov, *J. Fluid Mech.* **243**, 595 (1992).
 [21] R. C. Aguirre and H. J. Catrakis, *J. Fluid Mech.* **540**, 39 (2005).
 [22] T. Gilliland, K. K. J. Ranga-Dinesh, M. Fairweather, S. A. E. G. Falle, K. W. Jenkins, and A. M. Savill, *Flow, Turbul. Combust.* **89**, 385 (2012).
 [23] J. Mi and R. A. Antonia, *Phys. Rev. E* **64**, 026302 (2001).
 [24] X. Shen and Z. Warhaft, *Phys. Fluids* **14**, 370 (2002).
 [25] X. Q. Jiang, H. Gong, J. K. Liu, M. D. Zhou, and Z. S. She, *J. Fluid Mech.* **569**, 259 (2006).
 [26] M. Xu, A. Pollard, J. Mi, F. Secretain, and H. Sadeghi, *Phys. Fluids* **25**, 035102 (2013).
 [27] J. Mi, R. C. Deo, and G. J. Nathan, *Phys. Rev. E* **71**, 066304 (2005).
 [28] J. Mi, M. Xu, and C. Du, *Meas. Sci. Technol.* **22**, 125401 (2011).
 [29] A. A. Townsend, *Aust. J. Chem.* **2**, 451 (1949).
 [30] S. Corrsin and A. L. Kistler, NACA Report No. 1244, 1955.
 [31] H. A. Becker, H. C. Hottel, and G. C. Williams, *J. Fluid Mech.* **30**, 285 (1964).
 [32] I. Wygnanski and H. Fiedler, *J. Fluid Mech.* **38**, 577 (1969).
 [33] R. A. Antonia, A. Prabhu, and S. E. Stephenson, *J. Fluid Mech.* **72**, 455 (1975).
 [34] R. W. Bilger, R. A. Antonia, and K. R. Sreenivasan, *Phys. Fluids* **19**, 1471 (1976).
 [35] T. B. Hedley and J. F. Keffer, *J. Fluid Mech.* **64**, 625 (1974).
 [36] R. E. Falco and C. P. Gendrich, in *Near-Wall Turbulence: 1988 Zoran Zarić Memorial Conference*, edited by S. J. Kline and N. H. Afgan (Hemisphere Publishing Corp., Washington, DC, 1990), pp. 911–931.
 [37] D. H. Zhang, Y. T. Chew, and S. H. Winoto, *Exp. Therm. Fluid Sci.* **12**, 433 (1996).
 [38] S. B. Pope, in *Turbulent Flows* (Cambridge University Press, Cambridge, UK, 2000), p. 102.
 [39] H. Sadeghi and A. Pollard, in *Proceedings of the 7th International Symposium on Turbulence, Heat and Mass Transfer*, edited by Hanjalic, Nagano, and Jakirlic (Begell House Inc., New York, 2012).